

Synchrotron X-Ray Measurements of pMDI Sprays: Enabling Improved Nozzle Design

Daniel J. Duke¹, Nicholas Mason-Smith¹, Daniel Edgington-Mitchell¹,
Alan L. Kastengren², Jan Ilavsky², Paul Young³,
Daniela Traini³, David Lewis⁴ and Damon Honnery¹

¹ *Laboratory for Turbulence Research in Aerospace & Combustion,
Monash University, Melbourne, Victoria, Australia*

² *X-Ray Science Division, Argonne National Laboratory, Lemont IL 60439 USA*

³ *Respiratory Technology, Woolcock Institute of Medical Research and Discipline of
Pharmacology, School of Medicine, University of Sydney, New South Wales, Australia*

⁴ *Chiesi Limited, Chippenham UK*

*Keywords: synchrotron, X-ray, radiography, ultra-small angle X-ray scattering,
pressurized metered dose inhaler (pMDI), spray nozzle*

SUMMARY

In order to tailor the performance of pressurized metered dose inhalers (pMDIs) for a desired particle size distribution, the physical processes inside the spray and the nozzle must be understood in great detail. This necessitates non-invasive, in-situ particle and droplet size measurements. This article describes several X-ray diagnostic tools developed for this purpose. X-ray radiography measures the mass of liquid in the spray. X-ray fluorescence measures the drug distribution in the spray, independently of the propellant and any co-solvents. A new technique, ultra-small angle X-ray scattering, also provides a quantitative measurement of total surface area of liquid in the spray. These measurements are combined with traditional laser diffraction techniques to estimate important parameters which are difficult to directly measure, such as droplet composition and liquid volume distribution. Combining these measurement techniques allows us to observe the effects of pMDI formulation on the spray in much greater detail than has previously been possible. The measurements reveal the important role that nozzle exit

conditions and near-nozzle evaporative effects have on pMDI sprays, as the composition of the liquid droplets is found to vary significantly in the near nozzle region. A deeper understanding of these phenomena opens up new possibilities for the tailored design of pMDI devices for various drug and propellant combinations.

INTRODUCTION

The performance of pressurized metered dose inhalers (pMDIs) is dependent on the underlying spray physics and droplet formation processes [1]. Understanding the complex atomization mechanisms that occur in the actuator nozzle and determine droplet properties (e.g. size and velocity) is essential to the development of improved devices [2-6].

One of the challenges posed by the pMDI is the complex flow inside the device itself [6-7]. Figure 1 shows a series of false-color X-ray phase contrast images [7] of the gas-liquid flow inside a pMDI comprising 85% HFA-134a propellant and 15% ethanol. Color variations indicate the presence of complex gas-liquid structures that form as soon as the propellant begins to vaporize, which results in a complex multi-phase flow exiting the nozzle. Most diagnostic tools for evaluating pMDI performance are designed to operate far away from the nozzle, and only provide information about the resulting particles rather than the generation process. Given this constraint, empirical optimization of pMDI formulations has been advocated [8].

However, more insight can be obtained if measurements can be made closer to the nozzle, where it becomes possible to isolate phenomena and link design parameters to pharmaceutically relevant outcomes. To this end, a range of optical tools have been

applied to characterize aerosols generated by pMDIs [9-12], typically measuring velocity and size. However, the droplet composition remains unknown.

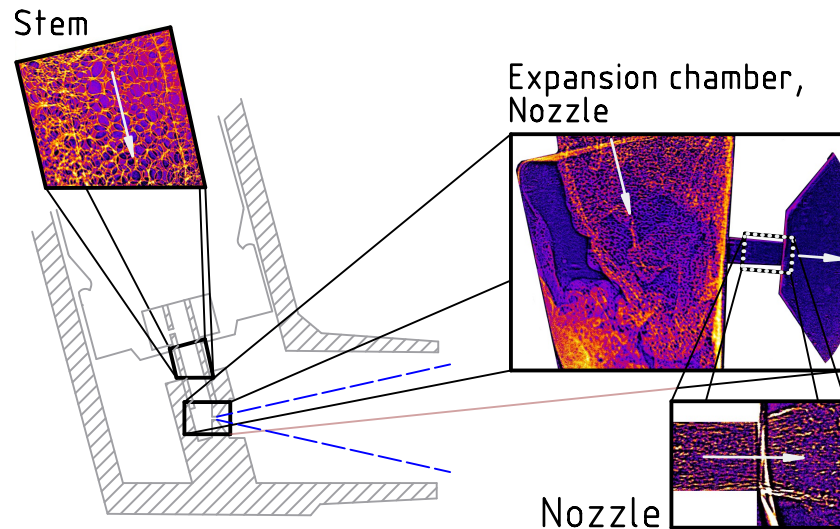


Figure 1. False-color X-ray phase contrast images reveal the complexity of the internal fluid flow in the stem, expansion chamber and nozzle region of an 85% HFA 134a, 15% ethanol pMDI spray. Changes in color are indicative of complex multi-phase flow.

A range of X-ray diagnostics for sprays [13] have also been adapted recently to the study of pMDIs [2,6,15]. X-ray radiography has been used to investigate density [2]; X-ray fluorescence has been used to characterize drug concentration [15], and phase-contrast imaging has been used to assess flow morphology [7; Figure 1].

This article introduces another X-ray technique, ultra-small angle X-ray scattering (USAXS) [16] which has recently been used to characterize droplet size of dense fuel sprays [17]. USAXS provides a quantitative measurement of total surface area of liquid in a spray and when these measurements are coupled with those from laser diffraction, X-ray fluorescence and X-ray radiography, can be used to estimate droplet composition and liquid volume distribution, which are difficult to measure directly.

ELECTRONIC METERED INHALER

Figure 2 illustrates the electronically metered inhaler (EMI) which was developed to provide repeatable and controlled conditions for the various measurements [2]. A nylon nozzle with an orifice diameter of 0.33 mm was cut from a Bepak inhaler actuator and connected to a programmable, micro-solenoid valve, which was connected to an unmetered canister that provided a continuous flow of formulation, whenever the valve was activated. The electronic valve allowed the spray to be formed with accurate and precise timing, with remote triggering. A 30 L/min flow of nitrogen was used to simulate inhalation. The nozzle assembly was mounted on a cylindrical chamber fitted with polyimide windows. The mouthpiece was also fitted with polyimide windows, so the flow could be directly observed all the way to the nozzle exit. Two formulations manufactured in house were investigated; 1 $\mu\text{g}/\mu\text{L}$ ipratropium bromide (IPBr) and 15% v/v ethanol co-solvent in either HFA-134a or HFA-227 propellant. The main difference between these two formulations is their vapor pressure; 5.7 bar for HFA-134a based formulation and 3.9 bar for HFA-227 based formulation at 20°C.

Measurements were repeated along the centerline of the spray (vertical coordinate y in Figure 2) from the nozzle exit plane ($y = -11.6\text{mm}$) up to approximately 70 mm downstream of the mouthpiece (see Table 1). All the experiments were time-averaged over the steady-state period of the spray. The valve was opened for 50 ms, producing a spray that lasted approximately 150 ms. The steady state period was measured from X-ray radiography data relative to the valve timing. It was found to be 35 to 85 ms after start of injection for the HFA-134a formulation, and 70 to 90 ms for the HFA-227 formulation.

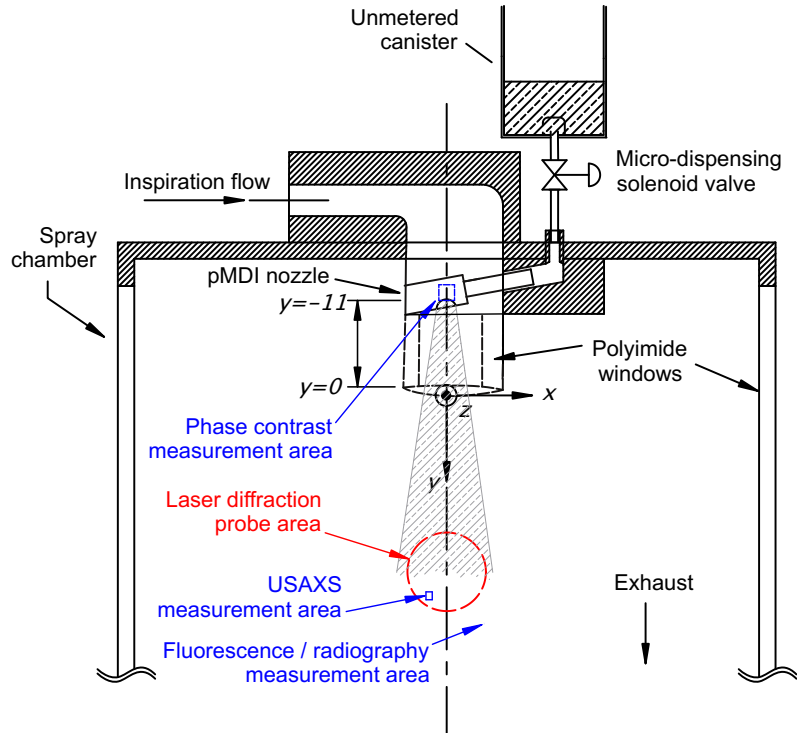


Figure 2. Schematic of electronic pMDI test facility. The various beam probe cross-sections areas for laser and X-ray experiments are shown (positions are arbitrary). Adapted from [2].

MEASUREMENT TECHNIQUES

Figure 3 illustrates the range of optical and X-ray measurement techniques used in this study [2,6]. Table 1 summarizes the key parameters of these techniques. Laser diffraction (LD) experiments were performed using a *Malvern Spraytec* particle sizer (Figure 3a) [18]. The Sauter mean diameter calculated from the droplet size distribution is related to the total surface area S and liquid volume V in the beam by $d_{32} = 6V / S$.

X-ray radiography (Figure 3b) and fluorescence (Figure 3c) measurements were performed at the 7-BM beamline of the Advanced Photon Source (APS), Argonne National Laboratory [19]. Briefly, a monochromatic X-ray beam is focused to a small spot at the mid plane of the spray. A time-series is recorded at a point and the spray is

translated through the beam. This is repeated many times to provide an ensemble average, spatially and temporally resolved measurement.

	Laser Diffraction (LD)	X-ray Radiography	X-ray Fluorescence	Ultra-Small Angle X-ray Scattering
Quantity Measured	Size Distribution, Approx. Volume	Aerosol Mass per Unit Area	Drug Mass per Unit Area	Liquid Surface Area per Unit Area
Light Source	670nm Laser	6 keV X-rays	15 keV X-rays	12 keV X-rays
Probe Area	1 cm Diameter	$5 \times 6 \mu\text{m}$	$5 \times 6 \mu\text{m}$	0.8 mm (transverse) \times 1.0 mm (axial)
Time Resolution	0.4 ms	$3.68 \mu\text{s}$	1 ms	Time-average during Steady State
Measurement Locations (axial)	-11 to +45 mm	-11 to +50 mm	-15 to +71.5 mm	-11, -10, -5, +5 mm
Sample Size	10	16	200	240
Time Required per Measurement	30 min	5 min	35 min	50 min

Table 1. Key parameters for the optical and X-ray measurement techniques.

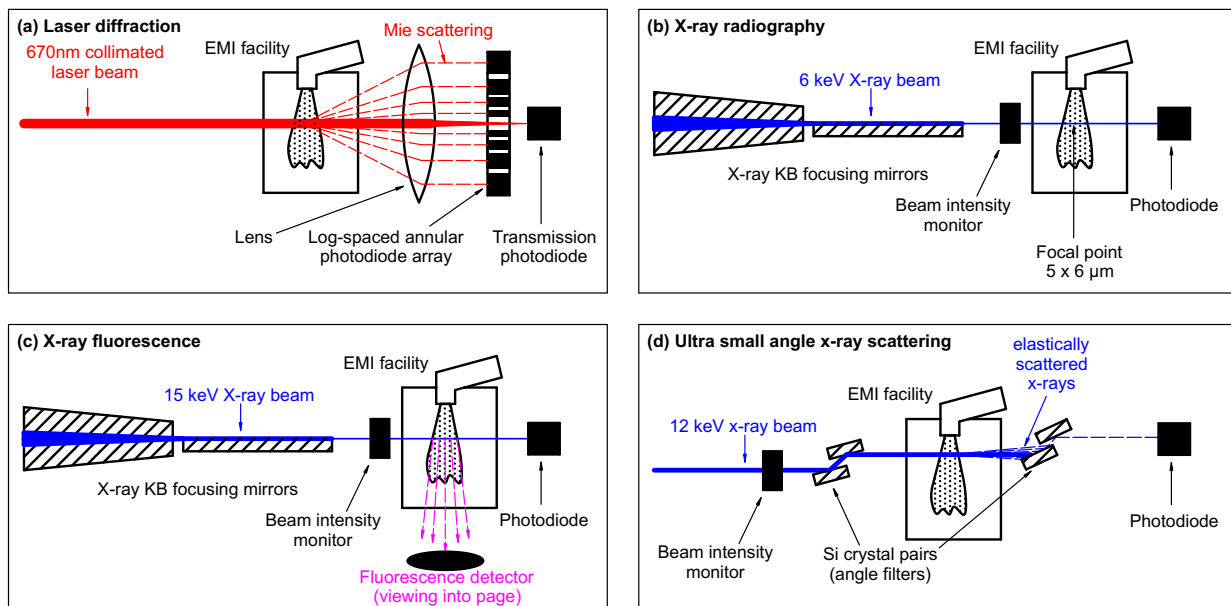


Figure 3. Simplified schematics of (a) Laser Diffraction (b) X-ray Radiography, (c) X-ray Fluorescence and (d) Ultra-small Angle X-ray Scattering Techniques.

For the radiography measurements [2], X-ray transmission is recorded by a photodiode. By comparing the transmitted and incident intensities (I/I_0) the projected mass of all species i along the beam path (z axis) is given by the Beer-Lambert Law:

$$\frac{I}{I_0} = \prod_{i=0}^N e^{-\mu_i \int \rho_i dz} \quad \text{Equation 1}$$

where μ_i are the species X-ray absorption coefficients and ρ_i are the species densities. Equation 1 is more complex than the approach used in previous work [2] as it separates the constituent species in the formulation, rather than treating the fluid as a homogeneous mixture. The total projected mass M used in previous studies [2,6] is related to Equation 1 by $M = \int \sum \rho_i dz$. The absorption coefficients for the constituents vary from $\mu \approx 16 \text{ cm}^2/\text{g}$ for pure ethanol to $\mu \approx 30 \text{ cm}^2/\text{g}$ for pure propellant. For the radiography experiments an incident beam energy of 6 keV was used, which provides sufficiently low energy for the beam to be well absorbed but high enough to give sufficient total flux. For the fluorescence measurements, the beam energy was increased to 15 keV to excite fluorescent emission from the bromine atom in the drug (IPBr) [15]. A detector at right angles to the beam (Figure 3c) detected this emission ($I_{\text{fluor.}}$). The projected drug concentration along the line of sight of the beam can be calculated;

$$\int \rho_{\text{drug}} dz = \frac{\psi I_{\text{fluor.}}}{I_0 \tau f_d f_a} \quad \text{Equation 2}$$

Corrections are made to account for detection efficiency (ψ, f_d), absorption of the incident beam (f_a), and loss due to reabsorption in the surrounds (τ) [15]. The advantage of the fluorescence technique is that it is able to measure the projected drug concentration independently of all other components in the formulation. The characteristic emissions

from the Br atoms are X-rays which occur against a zero background [15]. The emission mechanism is generally insensitive to temperature, pressure, and valence state [15].

Figure 3d provides a simplified schematic of the ultra-small angle X-ray scattering (USAXS) technique. These measurements were performed at the 9-ID beamline of the APS at Argonne National Laboratory [16]. The facility uses a Bonse-Hart configuration, which is capable of reaching scattering angles an order of magnitude smaller than conventional instruments. For our application, this is equivalent to being able to probe length scales up to approximately 10 μm . A monochromatic 12 keV beam is passed through a pair of collimating crystals. When the beam passes through the spray, some X-rays are elastically scattered. The X-rays pass through a second set of crystals which act as an angle filter [17]. By moving the crystals through a range of angles, repeating the spray, and normalizing against the environment without the spray, a scattering intensity profile is obtained. For our experiment, the droplet radii are larger than length scale range probed by the instrument, and the measurements thus follow Porod's law;

$$\frac{d\Sigma}{d\Omega}(q) = 2\pi\Delta\rho_X^2 S q^{-4} \quad \text{Equation 3}$$

The known parameters in Equation 3 are q (the scattering vector) and $d\Sigma/d\Omega$, the differential cross-section, which is calculated from the measurements [20]. The unknowns are S , the surface area, and $\Delta\rho_X^2$, the scattering contrast of the droplets. Scattering contrast is a function of droplet composition [19]; it varies from approximately $6 \times 10^{21} \text{ cm}^{-4}$ in pure ethanol to $14 \times 10^{21} \text{ cm}^{-4}$ in pure propellant.

RESULTS AND DISCUSSION

Figure 4 summarizes the results from the laser and X-ray techniques inside and outside the mouthpiece of the electronically metered inhaler test facility for both HFA 134a and HFA 227 based formulations. Data are shown up to 25 mm from the mouthpiece and the data are time-average measurements across the duration of the spray (50 ms). The time-resolved LD data indicated that the droplet size distribution was steady during the spray. Time resolved radiography also indicated that the injected mass per unit area was also relatively steady (within 10% of the mean value). The error bars in Figure 4 represent the uncertainty in the data due to both experimental error and fluctuation of the measurements about the ensemble mean values during the steady state period.

The LD data (Figure 4a) indicate that the Sauter mean diameter is slightly higher closer to the nozzle but remains relatively steady as the measurement moves downstream. Due to the large size of the probe area relative to the size of the spray, the LD data are subject to significant spatial averaging. The radiography data (Figure 4b) shows that the projected mass drops with increasing distance from the nozzle as the spray evaporates. However, the fluorescence data (Figure 4c) show the drug concentration along the beam path remains relatively constant with distance from the nozzle. This is expected, as conservation of total drug mass will give a constant projected density once integrated along the line of sight at the mid-plane. The USAXS measurement (Figure 4d) shows the surface area decreasing monotonically, similar to the radiography measurements.

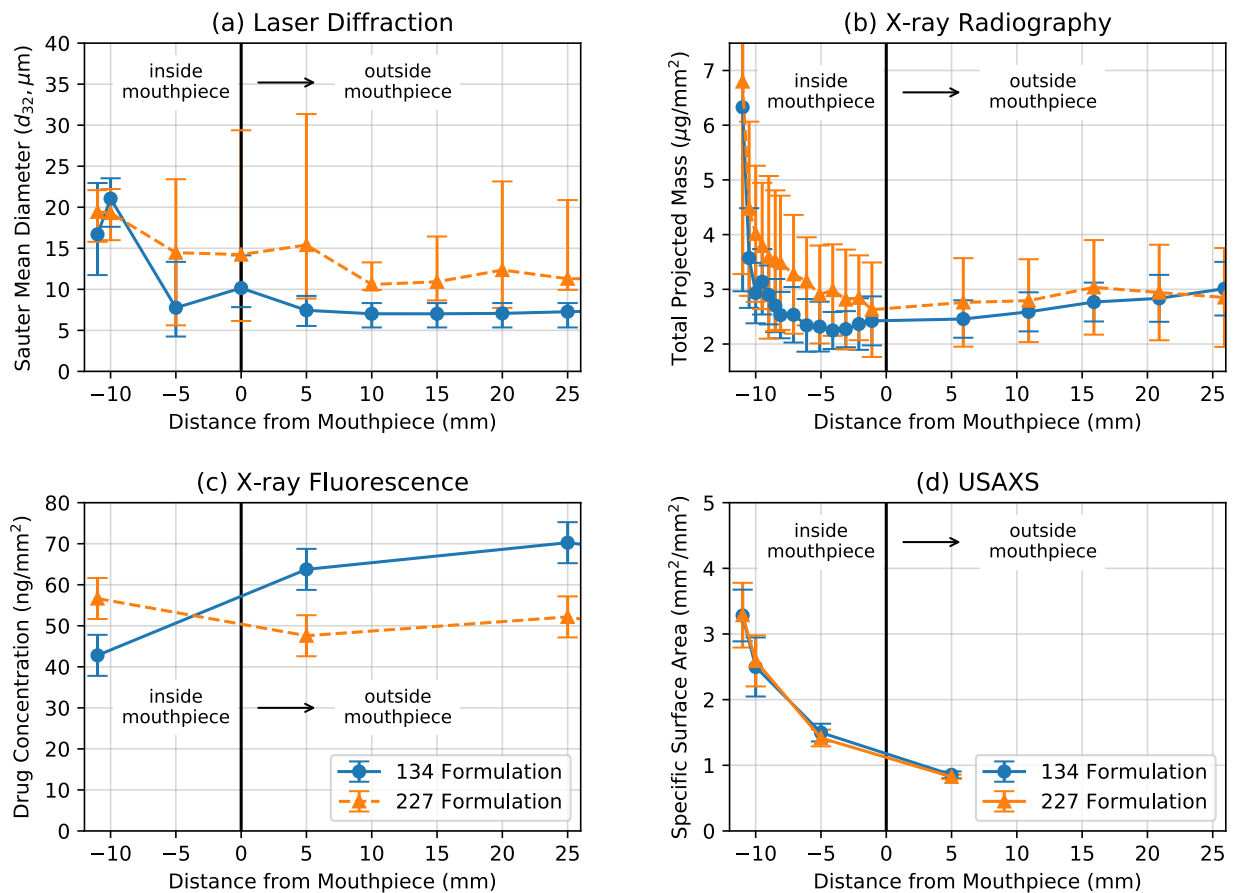


Figure 4. Measurements obtained using (a) laser and (b-d) X-ray techniques in the electronically metered inhaler facility for $1\mu\text{g}/\mu\text{L}$ IPBr, 15% ethanol, HFA 134a and $1\mu\text{g}/\mu\text{L}$ IPBr, 15% ethanol, HFA 227 formulations. All data are measured along the centerline axis of the spray with the horizontal co-ordinate indicating distance from the end of the mouthpiece. The nozzle exit is located at the leftmost end of the horizontal axis.

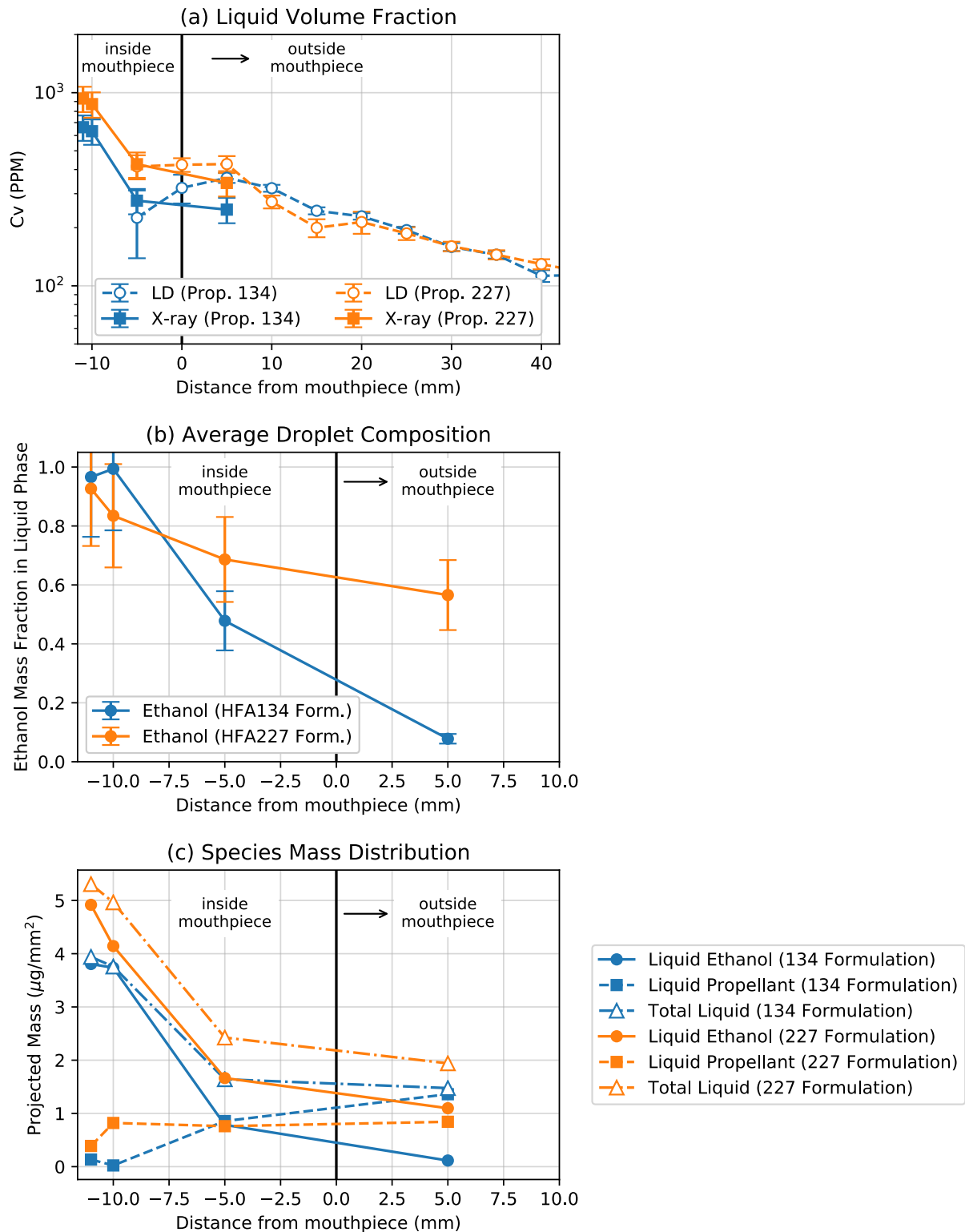


Figure 5. Calculated properties of metered-dose inhaler sprays derived from combined laser diffraction (LD) and X-ray measurements, for both 1µg/µL IPBr, 15% ethanol and HFA 134a and 227 formulations. All data are measured along the centerline axis of the spray with the horizontal co-ordinate indicating distance from the mouthpiece.

Figures 4 c-d are calculated assuming that the droplet composition (i.e. ratio of propellant to ethanol remaining in the liquid phase) matches that of the fluid inside the canister. However, the ethanol and propellant evaporate at different rates. Rather than assuming a composition, we can combine our measurements into a unified model with variable composition. The sensitivity of the X-ray techniques to the effects of composition can be exploited in order to solve for it. The model estimates line of sight integrated species volume fractions both in the droplets and the vapor phase which require the surface area in Equation 3 and the volume from Equation 1 to agree with the measured d_{32} , while conserving mass. Equations 1-3 are combined into a nonlinear system which is iteratively solved using non-linear least squares until it converges to within experimental uncertainty.

Figure 5a shows the resulting liquid volume fraction loading as a function of distance from the mouthpiece. Circles indicate an empirical estimate from the LD data alone. Squares indicate the volume loading calculated from the model. The X-ray data is utilized where the LD fails (around $y=5$ mm) due to excessive multiple scattering. Figures 5b and 5c show the composition of the liquid phase estimated by the model. The error bars indicate the sensitivity of the result to the uncertainty of the experimental data. Figure 5b suggests that the droplets exiting the nozzle are composed primarily of ethanol. As they evaporate, the relative ethanol concentration decreases. Species concentrations (Figure 5c) suggest that this is due to preferential evaporation of ethanol. This is surprising, as it suggests that the small amount of volatile propellant that still exists in the liquid phase upon exiting

the nozzle remains trapped in the droplets for a considerable time while the ethanol evaporates from the droplet surface. It should be noted that the USAXS measurement is sensitive to the surface concentration of the droplets, but in this preliminary investigation we have assumed the droplets are homogeneous. Both formulations exhibit comparable behaviour, but Figure 5b shows that the effect is more pronounced for the HFA 134a formulation. This is because fraction of liquid propellant at the nozzle exit is lower for HFA 134a (Figure 5c). The underlying reason for this lower liquid fraction is unclear and requires further investigation.

CONCLUSION

The adaption of a suite of synchrotron X-ray techniques to the study of pMDIs has revealed useful insights into the complex processes taking place in these devices. Each technique measures a different physical quantity, making them complementary to conventional approaches. These techniques can be combined to measure important pharmaceutically relevant parameters governing the environment in which the drug particles form. By combining a novel USAXS measurement with laser diffraction, X-ray radiography and fluorescence, it is possible to non-invasively characterize properties such as droplet composition, which cannot presently be obtained by other means.

Preliminary results reveal surprising behavior in the spray. Within millimeters of the nozzle, ethanol co-solvent appears to be predominant in the liquid state and evaporates preferentially to the propellant, some of which remains trapped inside the droplets. Since the drug is soluble in the ethanol and not the propellant, this implies that the drug distribution inside the droplets themselves may be heterogeneous and this may have

significant implications for the formation of drug particles. However, these results depend on a number of assumptions that require further testing. A preliminary understanding of these complexities suggests that pMDI nozzles may be modified to exploit this behavior. For example, changing the shape of the nozzle will alter the nozzle exit conditions. Differences in near nozzle conditions between the formulations suggest that the development of the spray and the rate of evaporation is sensitive to these conditions.

The insights gained through a combined X-ray and optical approach provide insight on the underlying physics behind empirical models for pMDI performance. This deeper understanding helps identify which parameters have the greatest impact on performance, and could be used to guide the future development of more efficient pMDIs.

ACKNOWLEDGEMENTS

Experiments were performed at the 7-ID, 7-BM and 9-ID beam lines of the APS at Argonne National Laboratory. Experiments at 7-BM and 9-ID were supported by DOE LDRD funding (Project No. 2017-098-N0). Use of the APS is supported by the U.S. Department of Energy (DOE) under Contract No. DE-AC02-06CH11357. The authors wish to thank Agilent Technologies for access to the LD equipment. The authors acknowledge funding support from the Australian Research Council (DE170100018, LP160101845). This research/project was undertaken with the assistance of resources and services from the National Computational Infrastructure (NCI), which is supported by the Australian Government.

REFERENCES

1. Clark AR: MDIs: Physics of Aerosol Formation. *J Aerosol Med* 1996, 9:19-26.
2. Mason-Smith N, Duke DJ, Kastengren AL, Stewart PJ, Traini D, Young PM, Chen Y, Lewis DA, Soria J, Edgington-Mitchell D, Honnery D: Insights into Spray Development from Metered-Dose Inhalers Through Quantitative X-ray Radiography. *Pharm Res* 2016, 33(5): 1249-1258.
3. Dunbar CA: Atomization Mechanisms of the Pressurized Metered Dose Inhaler. *Particulate Science and Technology* 1997, 15 (3-4): 253-271.
4. Chen Y, Young PM, Murphy S, Fletcher DF, Long E, Lewis D, Church T and Traini D: High-Speed Laser Image Analysis of Plume Angles for Pressurised Metered Dose Inhalers: The Effect of Nozzle Geometry. *AAPS PharmSciTech* 2017, 18(3): 782-789.
5. Ivey JW, Bhambri P, Church TK, Lewis DA, McDermott MT, Elbayomy S, Finlay WH and Vehring R: Humidity affects the morphology of particles emitted from beclomethasone dipropionate pressurized metered dose inhalers. *Int J Pharmaceutics* 2017, 520(1-2): 207-215.
6. Honnery D, Mason-Smith N, Duke DJ, Kastengren AL, Chen Y, Young PM, Traini D, Lewis DA, and Edgington-Mitchell, D: New insights into pMDI operation using synchrotron x-ray techniques. In *Respiratory Drug Delivery Asia 2016*. Edited by Dalby RN, Peart J, Young PM, Traini D. DHI Publishing; River Grove, IL: 2016: 209-220.
7. Mason-Smith N, Duke DJ, and Edgington-Mitchell D: High-speed X-ray imaging of Pressurized Metered-dose Inhaler Sprays with Variable Ethanol Content. In Proc. ILASS-Asia 2017, Jeju, Korea.
8. Lewis DA: A Priori Design of Metered Dose Inhalers. In *Respiratory Drug Delivery Asia 2016*. Edited by Dalby RN, Peart J, Young PM, Traini D. DHI Publishing; River Grove, IL: 2016: 187-198.
9. Buchmann NA, Duke DJ, Shakiba SA, Mitchell DM, Stewart PJ, Traini D, Young PM, Lewis DA, Soria J, Honnery D: A Novel High-Speed Imaging Technique to Predict the Macroscopic Spray Characteristics of Solution Based Pressurised Metered Dose Inhalers. *Pharm Res* 2014, 31(11): 2963-2974.
10. Alatrash A and Matida E: Characterization of Medication Velocity and Size Distribution from Pressurized Metered-Dose Inhalers by Phase Doppler Anemometry. *J Aerosol Med and Pulm Drug Deliv* 2016, 29(6): 501-513.
11. Versteeg HK, and Hargrave GK: Seeing is believing: Using optical diagnostics to investigate metered dose inhaler sprays and dry powder inhaler fluidization. In *Respiratory Drug Delivery Asia 2016*. Edited by Dalby RN, Peart J, Young PM, Traini D. DHI Publishing; River Grove, IL: 2016: 199-208.
12. Liu X, Doub WH and Guo, C: Evaluation of metered dose inhaler spray velocities using Phase Doppler Anemometry (PDA). *Int J Pharmaceutics* 2012, 423(2): 235-239.

13. Duke D, Swantek A, Kastengren A, Fezzaa K, and Powell C: Recent Developments in X-ray Diagnostics for Cavitation. *SAE Int. J. Fuels Lubr* 2015, 8(1): 135-146.
14. Swantek A, Kastengren A, Duke DJ, Tilocco Z, Sovis N and Powell C: Quantification of Shot-to-Shot Variation in Single Hole Diesel Injectors. *SAE Int. J. Fuels Lubr* 2015. 8 (1): 160-166.
15. Duke DJ, Kastengren AL, Mason-Smith N, Chen Y, Young PM, Traini D, Lewis D, Edginton-Mitchell D, Honnery D: Temporally and Spatially Resolved X-ray Fluorescence Measurements of in-situ Drug Concentration in Metered-Dose Inhaler Sprays. *Pharm Res* 2016, 33(4): 816-825.
16. Ilavsky J, Jemian PR, Allen AJ, Zhang F, Levine LE and Long GG: Ultra-small-angle X-ray scattering at the Advanced Photon Source. *J Appl Crystallogr* 2009, 42: 469-479.
17. Kastengren A, Ilavsky J, Viera JP, Payri R, Duke DJ, Swantek A, Tilocco F, Sovis N and Powell C: Measurements of Droplet Size in Shear-Driven Atomization Using Ultra-Small Angle X-Ray Scattering. *Int. J. Multiphas. Flow* 2017, 92: 131-139.
18. Haynes A, Shaik MS, Krarup H, Singh M: Evaluation of the Malvern Spraytec with inhalation cell for the measurement of particle size distribution from metered dose inhalers. *J Pharm Sci* 2004 93(2): 349-363.
19. Kastengren A, Powell C, Arms D, Dufresne EM, Gibson H, Wang J: The 7BM beamline at the APS: A facility for time-resolved fluid dynamics measurements. *J. Synchrotron Rad* 2012, 19(4): 654-657.
20. Ilavsky J, and Jemian PR: Irena: Tool suite for modeling and analysis of small-angle scattering. *J. Appl. Cryst* 2009, 42: 347-353.